Asymptotic Performance Bound on Estimation and Prediction of Mobile MIMO-OFDM Wireless Channels

Adeogun, Ramoni

Published in:
2018 IEEE Wireless Communications and Networking Conference, WCNC 2018

DOI (link to publication from Publisher):
10.1109/WCNC.2018.8377005

Publication date:
2018

Document Version
Early version, also known as pre-print

Asymptotic Performance Bound on Estimation and Prediction of Mobile MIMO-OFDM Wireless Channels

Ramoni. O. Adeogun
Wireless Communication Networks (WCN) Section,
Department of Electronics Systems,
Aalborg University, Aalborg, Denmark
Email: dradeogun01@gmail.com

***Abstract*—In this paper, we derive an asymptotic closed–form expression for the error bound on extrapolation of doubly selective mobile MIMO wireless channels. The bound shows the relationship between the prediction error and system design parameters such as bandwidth, number of antenna elements, and number of frequency and temporal pilots, thereby providing useful insights into the effects of these parameters on prediction performance. Numerical simulations show that the asymptotic bound provides a good approximation to previously derived bounds while eliminating the need for repeated computation and dependence on channel parameters such as angles of arrival and departure, delays and Doppler shifts.**

***Index Terms*—MIMO-OFDM, channel estimation, interpolation, prediction, Cramer-Rao bound, multipath channel**

I. Introduction

The development of algorithms for the prediction of MIMO–OFDM channels [1]–[11] to mitigate performance degradation resulting from feedback delays in adaptive and limited feedback MIMO-OFDM systems have received considerable attention in recent times. In the design of these algorithms, the ability to compute the lower bound on the estimation and prediction error performance as a function of the channel and system parameters is essential in order to make appropriate design decisions. Moreover, these bounds serve as a basis upon which the performance of the different algorithms can be compared. However, there exist no closed–form expressions relating MIMO–OFDM channel estimation, interpolation and prediction performance to predictor design parameters such as number of antennas, number of samples in the observation segment, number of pilot subcarriers, number of paths and SNR.

In [12], closed–form expressions for the prediction error in SISO–OFDM channels were derived. Bounds on the interpolation of MIMO–OFDM channels were derived in [13] using a vector formulation of the Cramer–Rao bound for a function of parameters. Similar bounds for estimation and prediction were proposed in [14], [15]. Although these bounds are useful in their own way, their expressions are not easily interpretable. Moreover, their dependence on channel parameters necessitates averaging over several realizations of the channel resulting in high computational load particularly for large numbers of samples and antenna elements. An asymptotic expression for the bound on the prediction of narrowband MIMO channels was derived in [16].

In this contribution, we derive simple, readily interpretable closed–form expressions for the error bound on MIMO–OFDM channel prediction in the asymptotic limit of large number of samples and/or antennas. The bounds are applicable to pilot based channel estimation, interpolation and prediction. The dependence of these bounds on system parameters, but not on channel parameters, enables them to provide useful insight into system design considerations.

II. Channel Model

We consider a wideband ray–based MIMO channel model defined as [17, p. 43]

$$\mathbf{H}(t,\tau)=\sum_{z=1}^{Z}\alpha_z\mathbf{a}_{\mathrm{r}}(\mu_z^{\mathrm{r}})\mathbf{a}_{\mathrm{t}}^{T}(\mu_z^{\mathrm{t}})e^{j\omega_z t}\delta(\tau-\tau_z) \quad (1)$$

where Z is the number of paths, α_z and ω_z are the complex amplitude and radian Doppler frequency of the zth path and τ_z is the delay of the zth path. $\mathbf{a}_{\mathrm{r}}(\mu_z^{\mathrm{r}})$ and $\mathbf{a}_{\mathrm{t}}(\mu_z^{\mathrm{t}})$ are the receive and transmit array response vectors associated with the zth path, respectively, while μ_z^{r} and μ_z^{t} are the angular frequencies associated with the angles of arrival and departure of the zth path, respectively. Note that while (1) is valid for all antenna geometries, we will consider a uniform linear array (ULA) such that $\mathbf{a}_{\mathrm{r}}(\mu_z^{\mathrm{r}})$ is defined as

$$\mathbf{a}_{\mathrm{r}}(\mu_z^{\mathrm{r}})=[1 \quad e^{-j\mu_z^{\mathrm{r}}} \quad e^{-j2\mu_z^{\mathrm{r}}} \quad \dots \quad e^{-j(N-1)\mu_z^{\mathrm{r}}}]^T \quad (2)$$

with $\mu_z^{\mathrm{r}}=2\pi\delta_{\mathrm{r}}\sin\theta_z$. N is the number of receive antenna elements, δ_{r} is the inter element spacing of the receive array and θ_z is the angle of arrival of the zth path. The transmit array response vector, $\mathbf{a}_{\mathrm{t}}(\mu_z^{\mathrm{t}})$, is analogously defined by replacing N with M and μ_z^{r} with μ_z^{t} in (2). The frequency response of the channel is obtained via the Fourier transform of (1) as[1]

$$\mathbf{H}(t,f)=\sum_{z=1}^{Z}\alpha_z\mathbf{a}_{\mathrm{r}}(\mu_z^{\mathrm{r}})\mathbf{a}_{\mathrm{t}}^{T}(\mu_z^{\mathrm{t}})e^{j(\omega_z t-2\pi f\tau_z)} \quad (3)$$

[1]It should be noted that although the carrier frequency, f_c may be included in the delay term as in [14], it is omitted here since it only result in a shift in the phase of each path.

where f denotes the frequency variable. We assume that channel parameters are stationary over the region of interest and that no two paths share the same parameter set $\{\alpha_z, \mu_z^{\mathrm{r}}, \mu_z^{\mathrm{t}}, \omega_z, \tau_z\}$ but two or more paths may share any subset of the parameter set. Assuming that the system has perfect sample timing and a proper cyclic extension, the sampled frequency response can be expressed as

$$\mathbf{H}(p,q) = \sum_{z=1}^{Z} \alpha_z \mathbf{a}_{\mathrm{r}}(\mu_z^{\mathrm{r}}) \mathbf{a}_{\mathrm{t}}^{T}(\mu_z^{\mathrm{t}}) e^{j(p\nu_z - q\eta_z)} \tag{4}$$

where p and q denote the sample and subcarrier index, respectively. $\nu_z = \Delta t \omega_z$ and $\eta_z = 2\pi \Delta f \tau_z$ are the normalized Doppler frequency and normalized delay, respectively for symbol period Δt and subcarrier spacing Δf. We assume that there are Q equally spaced pilot subcarriers in every OFDM symbol and that P equally spaced pilot symbols are available for the estimation, interpolation and/or prediction. Let $U_f = \lceil N_{\mathrm{sc}}/Q \rceil$ and $U_t = \lceil N_{\mathrm{pilot}}/P \rceil$ denote the frequency spacing (measured in number of subcarriers) between adjacent pilot subcarrier and temporal spacing (in number of OFDM symbols) between adjacent pilot symbols, respectively. N_{sc} is the total number of used subcarriers and N_{pilot} is the number of OFDM symbols in the training segment. In order to avoid frequency and time domain aliasing, U_f and U_t are chosen such that $\Delta f \tau_{\max} U_f \leq 1$ and $2\Delta t \omega_{\max} U_t \leq 1$ [18], where $\tau_{\max}$ and $\omega_{\max}$ are the maximum path delay and Doppler frequency, respectively. We denote the frequency and time indices of the pilots as $q' = qU_f; \quad q = 0, 1, 2, \cdots, Q-1$ and $p' = pU_t; \quad p = 0, 1, 2, \cdots, P-1$, respectively. We represent entry (n, m) of (4) as

$$h(n,m,p,q) = \sum_{z=1}^{Z} \alpha_z e^{j(p\nu_z - (n-1)\mu_z^{\mathrm{r}} - (m-1)\mu_z^{\mathrm{t}} - q\eta_z)} \tag{5}$$

for all $n = 1, \cdots, N$, $m = 1, \cdots, M$ and $p = 0, \cdots, P-1$. We assume that for the purpose of channel estimation, interpolation and/or prediction, PQ samples of the channel frequency response are known either from channel estimation or measurement. In practice, the channel estimates contain an error resulting from noise and interference, which we model as a summation of the true channel and a noise term [13]

$$\hat{h}(n,m,p,q) = h(n,m,p,q) + w(n,m,p,q) \tag{6}$$

where $w \sim \mathcal{CN}(0, \sigma^2)$. We will henceforth remove the indices in parenthesis and denote $h(n,m,p,q)$ as h.

III. Asymptotic Error Bound

We now derive a simple and easily interpretable closed–from expression for the lower bound on prediction mean square error (MSE) in the asymptotic case of large N, M, P and/or Q. We assume that estimation, interpolation or prediction are based on estimation of the parameters of the channel using the available pilot channels followed by estimation, interpolation or prediction for the desired frequency or time location using the estimated parameters. Let the channel parameter vector be denoted as[2]

$$\boldsymbol{\Theta} = [\boldsymbol{\theta}_1, \boldsymbol{\theta}_2, \cdots, \boldsymbol{\theta}_Z] \tag{7}$$

where

$$\boldsymbol{\theta}_z = [\Re(\alpha_z) \quad \Im(\alpha_z) \quad \mu_z^{\mathrm{r}} \quad \mu_z^{\mathrm{t}} \quad \nu_z \quad \eta_z] \tag{8}$$

$\Re(\cdot)$ and $\Im(\cdot)$ denote the real and imaginary parts of the associated complex number, respectively. Since our model represents a non-linear function of the channel parameters, the mean square error bound (MSEB) can be found using the Cramer–Rao lower bound (CRLB) for functions of parameters [19]

$$\mathrm{MSEB}(p,q) = \sum_{n=1}^{N} \sum_{m=1}^{M} \frac{\partial h}{\partial \boldsymbol{\Theta}} [\mathbf{J}(\boldsymbol{\Theta})]^{-1} \frac{\partial h}{\partial \boldsymbol{\Theta}}^{H} \tag{9}$$

where $\mathrm{MSEB}(p,q) = \mathbb{E}[(\hat{\mathbf{h}}(p,q) - \mathbf{h}(p,q))^H (\hat{\mathbf{h}}(p,q) - \mathbf{h}(p,q))]$, $\mathbf{J}^{-1}(\boldsymbol{\Theta})$ is the CRLB on the variance of the channel parameter estimates. The Jacobian in (9) is given by

$$\frac{\partial h}{\partial \boldsymbol{\Theta}} = \left[\frac{\partial h}{\partial \boldsymbol{\theta}_1} \quad \frac{\partial h}{\partial \boldsymbol{\theta}_2} \quad \cdots \quad \frac{\partial h}{\partial \boldsymbol{\theta}_Z} \right] \tag{10}$$

$\mathbf{J}(\boldsymbol{\Theta})$ is the Fisher information matrix (FIM), entries of which can be evaluated element-wise using Bangs formula [19],

$$[\mathbf{J}(\boldsymbol{\Theta})]_{ij} = \mathrm{Tr}\left[\mathbf{C}^{-1} \frac{\partial \mathbf{C}}{\partial \boldsymbol{\Theta}_i} \mathbf{C}^{-1} \frac{\partial \mathbf{C}}{\partial \boldsymbol{\Theta}_j} \right] + 2\Re\left[\frac{\partial \mathbf{h}^H}{\partial \boldsymbol{\Theta}_i} \mathbf{C}^{-1} \frac{\partial \mathbf{h}}{\partial \boldsymbol{\Theta}_j} \right] \tag{11}$$

where $\mathbf{C}$ is the noise covariance matrix. We assume that the estimation noise is Gaussian such that $\mathbf{C} = \sigma^2 \mathbf{I}$, and thus (11) can be reduced to

$$[\mathbf{J}(\boldsymbol{\Theta})]_{ij} = \frac{2}{\sigma^2} \Re\left(\sum_{q=0}^{Q-1} \sum_{p=0}^{P-1} \sum_{n=1}^{N} \sum_{m=1}^{M} \frac{\partial h}{\partial \boldsymbol{\Theta}_i} \frac{\partial h}{\partial \boldsymbol{\Theta}_j}^{H} \right) \tag{12}$$

Following straightforward derivation, the partial derivatives with respect to each of the parameters can be shown to be

$$\frac{\partial h}{\partial \Re(\alpha_z)} = e^{j(p\nu_z - (n-1)\mu_z^{\mathrm{r}} - (m-1)\mu_z^{\mathrm{t}} - q\eta_z)} \tag{13}$$

$$\frac{\partial h}{\partial \Im(\alpha_z)} = j e^{j(p\nu_z - (n-1)\mu_z^{\mathrm{r}} - (m-1)\mu_z^{\mathrm{t}} - q\eta_z)} \tag{14}$$

$$\frac{\partial h}{\partial \mu_z^r} = -j(n-1)\alpha_z e^{j(p\nu_z - (n-1)\mu_z^{\mathrm{r}} - (m-1)\mu_z^{\mathrm{t}} - q\eta_z)} \tag{15}$$

$$\frac{\partial h}{\partial \mu_z^t} = -j(m-1)\alpha_z e^{j(p\nu_z - (n-1)\mu_z^{\mathrm{r}} - (m-1)\mu_z^{\mathrm{t}} - q\eta_z)} \tag{16}$$

$$\frac{\partial h}{\partial \nu_z} = jpU_t \alpha_z e^{j(p\nu_z - (n-1)\mu_z^{\mathrm{r}} - (m-1)\mu_z^{\mathrm{t}} - q\eta_z)} \tag{17}$$

$$\frac{\partial h}{\partial \eta_z} = -jqU_f \alpha_z e^{j(p\nu_z - (n-1)\mu_z^{\mathrm{r}} - (m-1)\mu_z^{\mathrm{t}} - q\eta_z)} \tag{18}$$

[2]Note that although the noise variance σ^2 can also be included as an element of $\boldsymbol{\Theta}$, it is omitted here since this does not affect the expression for the prediction error bound.

Using (12) and (13)–(20) and performing some simplifications, the FIM submatrix corresponding to the zth path is obtained as

$$[\mathbf{J}(\boldsymbol{\theta}_z)] = \frac{NMPQ}{\sigma^2}\mathbf{K} \tag{19}$$

with

$$\mathbf{K} = \begin{bmatrix} 2 & 0 & 0 & 0 & 0 & 0 \\ 0 & 2 & 0 & 0 & 0 & 0 \\ 0 & 0 & \frac{2N^2}{3} & \frac{NM}{2} & -\frac{NPU_t}{2} & \frac{NQU_f}{2} \\ 0 & 0 & \frac{NM}{2} & \frac{2M^2}{3} & -\frac{MPU_t}{2} & \frac{MQU_f}{2} \\ 0 & 0 & -\frac{NPU_t}{2} & -\frac{MPU_t}{2} & \frac{2P^2U_t^2}{3} & -\frac{QPU_tU_f}{2} \\ 0 & 0 & \frac{NQU_f}{2} & \frac{MQU_f}{2} & -\frac{QPU_tU_f}{2} & \frac{2Q^2U_f^2}{3} \end{bmatrix} \tag{20}$$

where we have assumed that P, Q, N and/or M are large[3]. Similar to [14], [15] we assume that the complex amplitude is $\alpha_z \sim \mathcal{CN}(0,1)$, such that $\mathbb{E}[|\alpha_z|^2] = 1$ and $\mathbb{E}[\Re(\alpha_z)] = \mathbb{E}[\Im(\alpha_z)] = 0$. Using the structure of (19), the inverse of the FIM submatrix is given by

$$[\mathbf{J}(\boldsymbol{\theta}_z)]^{-1} = \frac{\sigma^2}{NMPQ}\mathbf{K}^{-1} \tag{21}$$

where $\mathbf{K}^{-1}$ is the inverse of $\mathbf{K}$ given by

$$\mathbf{K}^{-1} = \begin{bmatrix} \frac{1}{2} & 0 & 0 & 0 & 0 & 0 \\ 0 & \frac{1}{2} & 0 & 0 & 0 & 0 \\ 0 & 0 & \frac{60}{13N^2} & \frac{-18}{13MN} & \frac{18}{13NPU_t} & \frac{-18}{13NQU_f} \\ 0 & 0 & \frac{-18}{13MN} & \frac{60}{13M^2} & \frac{18}{13MPU_t} & \frac{-18}{13MQU_f} \\ 0 & 0 & \frac{18}{13NPU_t} & \frac{18}{13MPU_t} & \frac{60}{13P^2U_t^2} & \frac{18}{13PQU_tU_f} \\ 0 & 0 & \frac{-18}{13NQU_f} & \frac{-18}{13MQU_f} & \frac{18}{13PQU_tU_f} & \frac{60}{13Q^2U_f^2} \end{bmatrix} \tag{22}$$

Assuming that the scattering sources are uncorrelated, the FIM has a block diagonal structure

$$[\mathbf{J}(\boldsymbol{\Theta})] = \text{blkdiag}[\mathbf{J}(\boldsymbol{\theta}_1) \quad \mathbf{J}(\boldsymbol{\theta}_2) \quad \cdots \quad \mathbf{J}(\boldsymbol{\theta}_Z)] \tag{23}$$

The variance of the parameter estimates are therefore bounded by the diagonal entries of (23). Due to the diagonal structure of the FIM and independence of the FIM submatrices on path parameters, the asymptotic mean square error bound (AMSEB) can be written as

$$\text{AMSEB}(p,q) = \sum_{n=1}^{N}\sum_{m=1}^{M} \frac{\partial h}{\partial \boldsymbol{\Theta}}[\mathbf{J}(\boldsymbol{\Theta})]^{-1}\frac{\partial h}{\partial \boldsymbol{\Theta}}^H \tag{24}$$

For our analysis, we define the signal–to–noise ratio (SNR) as[4] $\text{SNR} = Z/\sigma_Z^2$. Thus, at the same SNR, the noise variance for a Z-path channel is $\sigma_Z^2 = Z\sigma^2$, where σ^2 is the noise variance for a single path channel. Substituting (21) into (24) and performing some simplifications, we obtain

$$\text{AMSEB}(p,q) = \frac{Z^2\sigma^2}{13PQ}\left[44 - \frac{36p}{PU_t} + \frac{60p^2}{P^2U_t^2} - \frac{36q}{QU_f} + \frac{60q^2}{Q^2U_f^2} - \frac{36qp}{P^2U_t^2Q^2U_f^2}\right] \tag{25}$$

Based on the assumption of normally distributed complex amplitudes, it can be shown that for a Z-path channel $\mathbb{E}[||\mathbf{H}||_F^2] = NMZ$ and the asymptotic normalized mean square error bound (ANMSEB) is obtained from (25) as

$$\text{ANMSEB}(p,q) = \frac{Z\sigma^2}{13NMPQ}\left[44 - \frac{36p}{PU_t} + \frac{60p^2}{P^2U_t^2} - \frac{36q}{QU_f} + \frac{60q^2}{Q^2U_f^2} - \frac{36pq}{QU_fPU_t}\right] \tag{26}$$

In this form, the ANMSEB provides useful insights on the effects of the number of antennas, number of frequency and time domain pilots, pilot spacing and SNR on the estimation, interpolation and prediction performance. The following observations can be made from (26):

- The subcarriers near the edge of the frequency band are less predictable than those near the centre.
- The NMSE grows linearly with an increasing noise variance σ^2 and number of propagation paths Z. This is intuitive and agrees with previous results that prediction becomes more difficult with increasing number of paths [20].
- The NMSE decreases with increasing number of antennas at either or both ends of the link. This is also intuitive since more structure of the channel is revealed by having more antennas.
- The contribution to the NMSE from the Doppler frequency (see (19),(26)) and delay estimation (see (20), (26)) lead to the p^2 and q^2 terms, respectively, demonstrating a quadratic increase with prediction horizon and with frequency. This shows the need to accurately estimate the Doppler frequency and path delays for spatial/temporal prediction and frequency domain interpolation, respectively.
- The contributions from the cross correlation of error terms involving the Doppler frequency lead to the negative linear term in p in (28), thus reducing the ANMSEB. A plausible explanation for this is that improved Doppler frequency estimates can be obtained from joint parameter estimation. A similar term is obtained from cross terms involving the delays.

IV. Numerical Simulations

In this section, we study the effects of system parameters on the error bounds and compare the asymptotic bound in (25) with the results in [14], [15]. In order to be consistent with [14], [15], we consider the root normalized mean square error (RNMSE) defined as $\text{RNMSE} = \sqrt{\text{NMSE}}$. The bound is averaged over 1000 independent channel realizations. We consider a MIMO-OFDM system with bandwidth

[3]It should be noted that P, Q, N and M do not all have to be large. We only require $NMPQ$ to be fairly large so that the approximation $NMPQ\mathbb{E}[g] \approx \sum_{i=1}^{NMPQ} g$ holds.

[4]This definition is necessary in order to allow fair comparison of the bound across channels with different number of paths

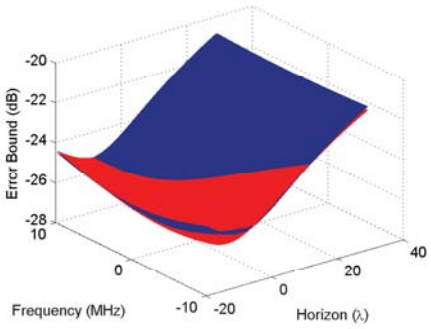

Fig. 1: Plot of RNMSE versus frequency and horizon (λ). The upper (blue) surface is the bound in [15] and the lower (red) surface is obtained using (26).

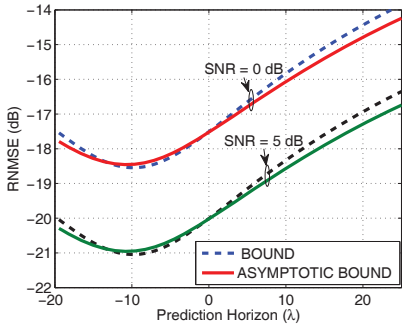

Fig. 2: Averaged RNMSE versus horizon (λ)

$B = 20\,\text{MHz}$, number of subcarriers $N_{\text{sc}} = 2048$ and 64 equally spaced pilot subcarriers. We assume that the channel is sampled at every symbol duration ($U_t = 1$). The complex amplitudes are drawn from $\alpha_z \sim \mathcal{CN}(0,1)$, the angles of arrival and departure are both chosen from a uniform distribution as $\theta_z^{\text{r}}, \theta_z^{\text{t}} \sim \mathcal{U}[-\pi, \pi)$ and the Doppler frequencies are generated from a spatial point of view as $\nu_z = 2\pi\Delta x \sin\theta_z^{\text{v}}$, where Δx is the spatial sampling interval in wavelengths and $\theta_z^{\text{v}} \sim \mathcal{U}[-\pi, \pi)$ is the angle between the direction of travel of the mobile station and the receive antenna array. The path delays are selected from the delays for the Urban macro (UMA) scenario in the WINNER II/3GPP channel [21]. We use $\Delta x = 0.2$ for our simulations.

Fig. 1 presents a plot of the asymptotic bound and the bounds in [14], [15] for a two path channel with $P = 100$, $Q = 64$, $N = 2$, $M = 2$ and $\text{SNR} = 15\,\text{dB}$ as a function of frequency and horizon (in wavelengths). As seen from the figure, the NMSE bounds increase quadratically in both frequency and temporal horizon and the asymptotic bound approximates the bound very closely.

In Fig. 2, we plot the RNMSE bounds averaged over frequency versus prediction horizon at $\text{SNR} = [0, 5]\,\text{dB}$. We observe that over the range considered, the maximum difference between the bounds in [14], [15] and our approximation is only about 0.3 dB. As expected the bounds increase with horizon but decreases with increasing SNR.

We plot the RNMSE bound versus the number of samples

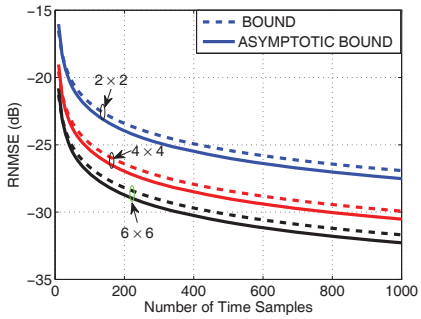

Fig. 3: Averaged RNMSE versus number of training samples.

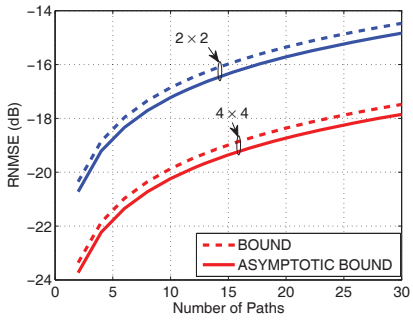

Fig. 4: Averaged RNMSE versus number of paths.

in the observation segment in Fig. 3 for different numbers of antenna elements at both ends of the link. We observe that, the RNMSE decreases with increasing number of samples. This is intuitively satisfying since an increased number of samples leads to improved parameter estimation and hence to better prediction. It also shows that an increase in the number of transmit and/or receive antenna decreases the RNMSE.

Finally, we show the effects of the number of paths on RNMSE in Fig. 4. We observe the the RNMSE bounds increases with increasing numbers of paths. This agrees with previous observations that propagation channel with dense multipath are more difficult to predict [20].

V. Conclusion

We have derived simple, easily interpretable and insightful closed–form expressions for the lower bounds on the performance of channel estimation, interpolation and prediction for MIMO–OFDM systems. The bound is obtained using the vector formulation of the Cramer Rao bound for functions of parameters in the asymptotic limits of large frequency and time–domain training samples and number of antennas. The expressions provide useful insights into the effects of system design parameters such as the number of antennas, number of training pilots, noise level, number of paths and pilot spacing on the error performance and are independent of the actual channel parameters. Simulation results show that the asymptotic error bound provides a good approximation to previous formulations while eliminating the need for repeated computation.

APPENDIX

Consider the expression for the FIM in (12) and assume that Q, P, N, and/or M are large such that

$$\sum_{q=0}^{Q-1}\sum_{p=0}^{P-1}\sum_{n=1}^{N}\sum_{m=1}^{M} h \approx QPNM\mathbb{E}[h] \tag{27}$$

Using (12) and (13), the diagonal entries of the FIM are obtained as

$$[\mathbf{J}]_{11} = [\mathbf{J}]_{22} = \frac{2QPNM}{\sigma^2} \tag{28}$$

$$[\mathbf{J}]_{33} = \frac{2}{\sigma^2}\left(MPQ(\sum_{n=1}^{N}(n-1)^2)\mathbb{E}[|\alpha_z|^2]\right) \tag{29}$$

$$[\mathbf{J}]_{44} = \frac{2}{\sigma^2}\left(NPQ(\sum_{m=1}^{M}(m-1)^2)\mathbb{E}[|\alpha_z|^2]\right) \tag{30}$$

$$[\mathbf{J}]_{55} = \frac{2}{\sigma^2}\left(NPQ(\sum_{k=0}^{P-1}(pU_t)^2)\mathbb{E}[|\alpha_z|^2]\right) \tag{31}$$

$$[\mathbf{J}]_{66} = \frac{2}{\sigma^2}\left(NPK(\sum_{q=0}^{Q-1}(qU_f)^2)\mathbb{E}[|\alpha_z|^2]\right) \tag{32}$$

Using the identity

$$\sum_{a=1}^{A} a^2 = \frac{A(A+1)(2A+1)}{6} \tag{33}$$

and our assumption that the complex amplitude is $\alpha_z \sim \mathcal{CN}(0,1)$, (28) becomes

$$\begin{aligned}
[\mathbf{J}]_{33} &= \frac{2}{\sigma^2}\left(\frac{MPQN(N-1)(2N-1)}{6}\right)\\
[\mathbf{J}]_{44} &= \frac{2}{\sigma^2}\left(\frac{NPQM(M-1)(2M-1)}{6}\right)\\
[\mathbf{J}]_{55} &= \frac{2}{\sigma^2}\left(\frac{NMQP(P-1)(2P-1)U_t^2}{6}\right)\\
[\mathbf{J}]_{66} &= \frac{2}{\sigma^2}\left(\frac{NMPQ(Q-1)(2Q-1)U_f^2}{6}\right)
\end{aligned} \tag{34}$$

Since $N, M, Q, P > 1$, the approximations $A-1 \approx A$ and $2A-1 \approx 2A$ can be used to simplify (34) as

$$\begin{aligned}
[\mathfrak{J}]_{33} &= \frac{NMPQ}{\sigma^2}\left(\frac{2N^2}{3}\right); \quad [\mathfrak{J}]_{44} = \frac{NMPQ}{\sigma^2}\left(\frac{2M^2}{3}\right)\\
[\mathfrak{J}]_{55} &= \frac{NMPQ}{\sigma^2}\left(\frac{2P^2U_t^2}{3}\right); \quad [\mathfrak{J}]_{66} = \frac{NMPQ}{\sigma^2}\left(\frac{2Q^2U_f^2}{3}\right)
\end{aligned} \tag{35}$$

The off-diagonal entries of the FIM are obtained following the same procedure.

ACKNOWLEDGMENT

The authour would like to thank Assoc. Prof. Paul D. Teal and Dr. Pawel A. Dmochowski at the School of Engineering and Computer Science, Victoria University of Wellington, New Zealand for their technical guidance, contributions and comments during the course of this research.

REFERENCES

[1] M. S. Kumar and S. Kirthiga, "Review of parametric radio channel prediction schemes for mimo system," in *2016 International Conference on Circuit, Power and Computing Technologies (ICCPCT)*, March 2016, pp. 1–5.

[2] L. Fan, Q. Wang, Y. Huang, and L. Yang, "Performance analysis of low-complexity channel prediction for uplink massive mimo," *IET Communications*, vol. 10, no. 14, pp. 1744–1751, 2016.

[3] R. Nagashima, T. Ohtsuki, W. Jiang, Y. Takatori, and T. Nakagawa, "Channel prediction for massive mimo with channel compression based on principal component analysis," in *2016 IEEE 27th Annual International Symposium on Personal, Indoor, and Mobile Radio Communications (PIMRC)*, Sept 2016, pp. 1–6.

[4] R. O. Adeogun, P. D. Teal, and P. A. Dmochowski, "Channel prediction for millimeter wave mimo systems in 3d propagation environments," in *2017 24th International Conference on Telecommunications (ICT)*, May 2017, pp. 1–5.

[5] Z. Xu, M. Hofer, and T. Zemen, "A time-variant channel prediction and feedback framework for interference alignment," *IEEE Transactions on Vehicular Technology*, vol. 66, no. 7, pp. 5961–5973, July 2017.

[6] J. Martyna, "Intelligent System for Channel Prediction in the MIMO-OFDM Wireless Communications Using a Multidimensional Recurrent LS-SVM," in *Proc. 8th International Conference on Hybrid Artificial Intelligent Systems*, 2013, pp. 441–450.

[7] R. O. Adeogun, P. D. Teal, and P. A. Dmochowski, "An adaptive parametric prediction method for mobile mimo wireless systems," in *2017 European Conference on Networks and Communications (EuCNC)*, June 2017, pp. 1–5.

[8] S. Uehashi, Y. Ogawa, T. Nishimura, and T. Ohgane, "Channel prediction using compressed sensing in multi-user mimo systems," in *2016 International Conference on Computing, Networking and Communications (ICNC)*, Feb 2016, pp. 1–6.

[9] M. B. Amin, W. Zirwas, and M. Haardt, "Advanced channel prediction concepts for 5g radio systems," in *2015 International Symposium on Wireless Communication Systems (ISWCS)*, Aug 2015, pp. 166–170.

[10] C. Min, N. Chang, J. Cha, and J. Kang, "MIMO-OFDM Downlink Channel Prediction for IEEE802.16e Systems Using Kalman Filter," in *Proc. IEEE Wireless Communications and Networking Conference*, 2007, pp. 942–946.

[11] R. O. Adeogun, P. D. Teal, and P. A. Dmochowski, "Novel algorithm for prediction of wideband mobile mimo wireless channels," in *Proc. IEEE International Conference on Communications*, June 2014.

[12] I. C. Wong and B. L. Evans, "Sinusoidal Modeling and Adaptive Channel Prediction in Mobile OFDM Systems," *IEEE Trans. on Sig. Proc.*, vol. 56, no. 4, pp. 1601–1615, 2008.

[13] M. Larsen, A. Swindlehurst, and T. Svantesson, "A Performance Bound for Interpolation of MIMO-OFDM Channels," in *Proc. Fortieth Asilomar Conference on Signals, Systems and Computers*, 2006, pp. 1801–1805.

[14] M. Larsen, L. Swindlehurst, and T. Svantesson, "A Performance Bound for MIMO-OFDM Channel Estimation and Prediction," in *Proc. Fifth IEEE Sensor Array and Multichannel Signal Processing Workshop*, 2008, pp. 141–145.

[15] M. D. Larsen, A. L. Swindlehurst, and T. Svantesson, "Performance bounds for MIMO-OFDM channel estimation," *IEEE Transactions on Signal Processing*, vol. 57, no. 5, pp. 1901–1916, May 2009.

[16] R. O. Adeogun, P. D. Teal, and P. A. Dmochowski, "Asymptotic Error Bounds on Prediction of Narrowband MIMO Wireless Channels," *IEEE Signal Processing Letters*, vol. 21, pp. 1103 – 1107, 2014.

[17] B. Clerckx and C. Oestges, *MIMO Wireless Networks: Channels, Techniques and Standards for Multi-Antenna, Multi-User and Multi-Cell Systems*, 2nd ed. Academic Press, 2013.

[18] H. Shirani-Mehr, D. Liu, and G. Caire, "Channel state prediction, feedback and scheduling for a multiuser mimo-ofdm downlink," in *42nd Asilomar Conference on Signals, Systems and Computers*, Oct 2008, pp. 136–140.

[19] S. M. Kay, *Fundamentals of statistical signal processing: estimation theory*. Upper Saddle River, NJ, USA: Prentice-Hall, Inc., 1993.

[20] P. Teal and R. Vaughan, "Simulation and performance bounds for real-time prediction of the mobile multipath channel," in *Proc. IEEE Workshop on Statistical Signal Processing Proceedings*, 2001, pp. 548–551.

[21] "IST-WINNER II Deliverable 1.1.2 v.1.2, WINNER II channel models," IST-WINNER2, Tech. Rep., 2007. [Online]. Available: http://www.ist-winner.org/deliverables.html